

Molecular Dynamics Simulation of an Argon Gas

Jorrit Hortensius (4240901) & Bas van 't Hooft (4217152)
Delft University of Technology

In this paper an argon gas consisting of particles interacting via the Lennard-Jones potential is simulated in both the microcanonical and canonical ensemble using molecular dynamics simulations. The Verlet algorithm is used to update the positions and velocities using the total force on each particle. From these simulations the heat capacity, pair correlation function and pressure are determined and compared with previous results. Furthermore, the diffusive behaviour of the system is characterized for various phases.

CONTENTS

I. Introduction	1
II. Model	1
A. Lennard-Jones Potential	1
B. Verlet Algorithm	2
C. Boundary Conditions	2
D. Initialization	3
E. Thermostat	3
F. Natural Units	3
G. Choice of Step-size	3
H. Data-blocking	4
III. Results	4
A. Heat capacity	4
B. Pair correlation function	4
C. Pressure	5
D. Diffusion	6
IV. Conclusion and Outlook	7
Appendix A. Error specific heat	7
References	7

tions to physical problems is called Computational Physics.

One of the problems which lends itself for computational physics, is the many-body problem of interacting particles. The solution to the resulting set of coupled differential equations can be approximated with the aid of a computer. In particular, the behaviour of an argon gas consisting of several hundreds of particles, has been used as a standard computational problem. In 1964 Loup Verlet, a pioneer in the computer simulation of molecular dynamics models, published the results of his simulations [1].

In this project, we are going to redo the classical simulation performed by Verlet many years ago. The goal of this research is to extract thermodynamic quantities from the simulation and compare them with theoretical values for limiting cases of solids and ideal gases.

In Section II the model is described. Using this model it is possible to calculate several thermodynamic quantities, which is discussed in Section III. Some theory is contained within this section to make it more self-contained. Then in Section IV we end with some concluding remarks.

I. INTRODUCTION

Solving a physical problem often comes down to solving a set of differential equations which mathematically describe the problem. In very simple cases, these problems admit an analytic solution. Subsequently, this mathematical solution helps us to understand the physics involved in the problem.

For many real-world problems, the corresponding equations cannot be solved analytically. However, we still want to get more insight in the physics. In these cases, we can call for computer assistance and try to approach the ‘real’ solution with numerical approximations. The approximations, if valid, help us to understand the problem, even though we cannot find the exact solution. The area dealing with numerical approxima-

II. MODEL

A. Lennard-Jones Potential

We would like to model N interacting argon atoms in a fixed volume V . It is assumed that those atoms only interact pairwise via the Lennard-Jones potential which depends on the distance between two particles, $r = |\mathbf{r}_i - \mathbf{r}_j|$. This potential models both hard core repulsion and dipole-dipole interaction. Hard core repulsion is caused by Pauli repulsion of overlapping electron orbitals at short ranges. This behaviour is modelled by the r^{-12} component of Eq. 1. The dipole-dipole interaction gives rise to the van der Waals force and can be described by the r^{-6} component of Eq. 1.

$$U(r) = 4\epsilon \left[\left(\frac{\sigma}{r} \right)^{12} - \left(\frac{\sigma}{r} \right)^6 \right] \quad (1)$$

The Lennard-Jones potential U has two parameters: ϵ , which describes the depth of the potential well and σ , which describes the range of the hard core repulsion. This is illustrated in Fig. 1. Experiments have shown that for argon $\epsilon = 1.65 \cdot 10^{-21}$ J and $\sigma = 3.4 \cdot 10^{-10}$ m are the best fitting parameters [2]. From Eq. 1 it can be found that the minimum of the potential r_m corresponds to $2^{1/6}\sigma$.

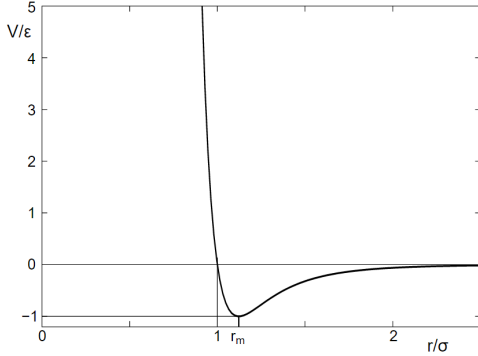


FIG. 1: Lennard-Jones potential (Eq. 1) as function of distance.[3]

The force on particle i is given by

$$\mathbf{F}_i = \sum_{\substack{j=1 \\ j \neq i}}^N -\nabla_i V(|\mathbf{r}_i - \mathbf{r}_j|) = \sum_{\substack{j=1 \\ j \neq i}}^N \mathbf{F}_{ij}. \quad (2)$$

If we would calculate the force on each particle with this equation then this would require $N(N-1)$ calculations of the force. However, using Newton's third law $\mathbf{F}_{ij} = -\mathbf{F}_{ji}$ the force on all the particles can be calculated using only $N(N-1)/2$ evaluations of the force, which is a significant speed-up.

In addition, the force is neglected if the particle pair is more than the cutoff distance $r_{co} = 3\sigma$ apart. This can be justified when looking at Fig. 1, where the gradient of the potential goes to zero for r large.

B. Verlet Algorithm

Once the force is known, we can calculate the position at a later time using a numerical procedure based on the Taylor-expansion

dure based on the Taylor-expansion

$$\begin{aligned} \mathbf{x}(t + \Delta t) &= \mathbf{x}(t) + \frac{d\mathbf{x}}{dt} \Big|_t \Delta t + \frac{1}{2} \frac{d^2\mathbf{x}}{dt^2} \Big|_t \Delta t^2 + \mathcal{O}(\Delta t^3) \\ \mathbf{x}(t + \Delta t) &= \mathbf{x}(t) + \mathbf{v}(t)\Delta t + \frac{\mathbf{F}(t)}{2m} \Delta t^2 + \mathcal{O}(\Delta t^3), \end{aligned} \quad (3)$$

where both the definition of velocity and Newton's second law were used. If the same approach is used for the velocity we obtain

$$\mathbf{v}(t + \Delta t) = \mathbf{v}(t) + \frac{\mathbf{F}(t)}{m} \Delta t + \mathcal{O}(\Delta t^2), \quad (4)$$

which is only valid up to order Δt^2 . This can be improved by combining

$$\begin{aligned} \mathbf{v}(t) &= \mathbf{v}(t + \Delta t) - \frac{\mathbf{F}(t + \Delta t)}{m} \\ &\quad + \frac{1}{2} \frac{d^2\mathbf{v}}{dt^2} \Big|_{t+\Delta t} \Delta t^2 + \mathcal{O}(\Delta t^3) \end{aligned} \quad (5)$$

$$\begin{aligned} \mathbf{v}(t + \Delta t) &= \mathbf{v}(t) + \frac{\mathbf{F}(t)}{m} \Delta t \\ &\quad + \frac{1}{2} \frac{d^2\mathbf{v}}{dt^2} \Big|_t \Delta t^2 + \mathcal{O}(\Delta t^3). \end{aligned} \quad (6)$$

If Eq. 5 is subtracted from Eq. 6 the following equation is obtained

$$\begin{aligned} \mathbf{v}(t + \Delta t) &= \mathbf{v}(t) + \frac{\Delta t}{2m} [\mathbf{F}(t + \Delta t) + \mathbf{F}(t)] \\ &\quad + \frac{\Delta t^2}{4} \left[\frac{d^2\mathbf{v}}{dt^2} \Big|_t - \frac{d^2\mathbf{v}}{dt^2} \Big|_{t+\Delta t} \right] + \mathcal{O}(\Delta t^3) \\ \mathbf{v}(t + \Delta t) &= \mathbf{v}(t) + \frac{\Delta t}{2m} [\mathbf{F}(t + \Delta t) + \mathbf{F}(t)] + \mathcal{O}(\Delta t^3), \end{aligned} \quad (7)$$

where we used that the difference in the second order derivatives itself is zero up to order Δt . Eq. 3 and 7 describe the Verlet algorithm, which is valid up to order Δt^3 . This numerical scheme is used in the current model.

C. Boundary Conditions

We cannot hope to simulate the number of particles present in most physically relevant systems. However, if the correct boundary conditions are used, the observed behaviour is the same as for much larger systems. In the large physically relevant systems the effects of the boundary are very limited. Therefore it is desired to simulate a small fraction of a larger container.

There are a multitude of possible choices for the boundary conditions for example fixed boundary conditions (FBC) and periodic boundary conditions (PBC). In FBC the particles are reflected when they hit the wall, whereas in PBC they move through the wall and end up at the opposite side of the container. In FBC the walls will strongly affect the behaviour of the gas and for this reason PBC are desired.

In addition the nearest image convention is used. By doing so we pretend that the system is surrounded by identical systems. Each particle interacts with all other particles, but only with the copy which is most nearby.

D. Initialization

Both the positions and velocities of all the particles have to be initialized before the simulation starts. It is desired to start close to an equilibrium situation as only a limited number of time-steps can be simulated. If an initial state very far from equilibrium would be chosen, then the simulation could last too long.

Argon has a fcc lattice in the solid state and the atoms are therefore initialized according to this lattice. The unit cell in the fcc lattice is shown below (Fig. 2).

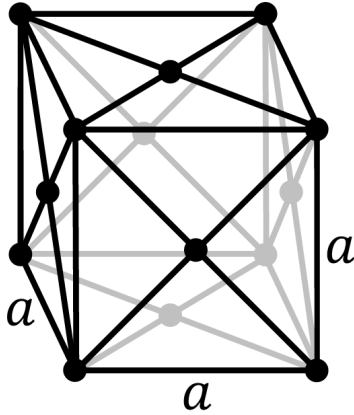


FIG. 2: Unit cell in the fcc lattice.[4]

The velocities are initialized according to the Maxwell-Boltzmann probability distribution:

$$f(\mathbf{v}) = \left(\frac{m}{2\pi k_B T}\right)^{3/2} \exp\left[-\frac{m(v_x^2 + v_y^2 + v_z^2)}{2k_B T}\right]. \quad (8)$$

Each component of the velocity is drawn from a normal distribution with variance $m/k_B T$. However, due to the small number of particles, the total initial velocity is not necessarily equal to zero in each direction. It is easier to study the system

when the total net velocity is zero, and thus the velocity of each particle is shifted to make the total momentum zero.

E. Thermostat

During the simulation the temperature can change since potential energy can be converted into kinetic energy. It is the kinetic energy which determines the temperature by the equipartition theorem. It is desired to model the system in the canonical ensemble, thus the temperature should be fixed. This can be done by multiplying the velocity of each particle by a factor such that the velocities satisfy the equipartition theorem for a fixed T. This factor is given by

$$\lambda = \sqrt{\frac{3(N-1)k_B T}{m \sum_{i=0}^{N-1} v_i^2}}. \quad (9)$$

F. Natural Units

In all sections below, natural units are used to streamline notation and calculations. This means that σ , ϵ , m and k_B are all set equal to 1. As a consequence, lengths are measured in units of σ , temperatures in $\epsilon/k_B = 120$ K and times in $\sigma(m/\epsilon)^{1/2} = 2.2$ ps.

The density $\rho = N/V$ is measured in units of $1/\sigma^3$. $n = 1$ corresponds to a packing where there is one particle per σ^3 . For a fcc lattice this makes that the nearest neighbours are coincidentally located at the minimum of the Lennard-Jones potential for $n = 1$.

G. Choice of Step-size

In this section the step-size for the Verlet algorithm is examined. Especially at high temperatures it is important that the atoms can move only a small fraction of σ during each timestep, as otherwise they could get too close, which in turn causes very high accelerations and thus inaccuracies. This can be made quantitative by requiring that the time-step is much smaller than the eigenfrequency of the potential well.

The eigenfrequency of the potential well is given by

$$\omega = \sqrt{\frac{1}{m} \left. \frac{d^2 V}{dr^2} \right|_{r_m}} = \sqrt{\frac{72\epsilon}{mr_m^2}} = \sqrt{\frac{72}{2^{(1/3)}}} \quad (10)$$

This results in a $T = 2\pi/\omega = 0.83$. This gives an indication of the relevant time scale. Keeping in mind that the Lennard-Jones potential is very skewed, much smaller time-steps have to be used. For this reason $\Delta t = 0.004$ is used in all simulations. In SI units this corresponds to time-steps of 8.6 fs. If the energy and the momentum are conserved during the simulations, this indicates that this is a suitable step-size.

H. Data-blocking

In this project, the values of several thermodynamic quantities will be determined by simulation. These values are determined as expectation values of physical quantities over time. The postulate of statistical mechanics is used, which states that for very long times, the time average of a physical quantity approaches the average over all configurations. The time average of quantity A after M steps is simply given by $\bar{A} = \sum_{i=1}^M A_i$, where A_i is the value at time-step i .

In general, the computation time and therefore the simulation time are limited, which can lead to small deviations in the time average compared to the ‘real’ system average. To get a grip on these errors, we have a look at the standard deviation σ of the physical quantity which is defined as

$$\sigma^2 = \langle A^2 \rangle - \langle A \rangle^2.$$

and is an intrinsic The expectation values can again be approximated by time-averages obtained in the simulation.

However, we are interested in the statistical error in the mean value of \bar{A} as well, which is determined during the simulation. The data of length M is chopped into blocks of size m . Each block needs to be longer than the correlation time, so that each block contains independent ‘configurations’ of the system. For each block the average value of the physical quantity is determined. By averaging over the different blocks and determining the standard deviation of these uncorrelated values, we obtain an estimate for both the physical quantity and the error. This method is called *data-blocking*. The block size has to be larger than the correlation length, while small enough to have enough blocks to obtain an accurate estimate of the standard deviation. A correct block size will be found by trial and error.

III. RESULTS

A. Heat capacity

The heat capacity of a system can be calculated from the fluctuations in the kinetic energy K using the Lebowitz formula[2]

$$C_V = \frac{3N}{2} \frac{1}{1 - \frac{3N\langle\delta K^2\rangle}{2\langle K \rangle^2}}, \quad (11)$$

where $\langle\delta K^2\rangle$ is the standard deviation squared of the kinetic energy. In the solid phase at low temperatures the Lennard-Jones potential can be approximated as a parabolic potential centered around r_{min} . In that case the solid can be approximated as $3N$ independent harmonic oscillators which satisfy the equipartition theorem. The resulting heat capacity C_V is approximately $3N$. In the gas phase at very low densities the argon gas can be approximated as an ideal gas, resulting in $C_V \approx 3N/2$.

Figure 3 shows the values for the specific heat found using Eq. 11. The specific heat is the heat capacity per particle $c_V = C_V/N$. These results were obtained using $N = 500$. To equilibrate the system in the canonical ensemble 5000 time-steps were used for $T \leq 1$ and 2000 time-steps for $T > 1$. Then the specific heat was determined in the canonical ensemble, such that kinetic energy can be converted into potential energy and vice versa. The fluctuations $\langle\delta K^2\rangle$ were obtained using data-blocking. Because the data-blocks have to be large for low temperature, the errors in the specific heat are large. This indicates that blocks longer than of length 1500 timesteps should have been used. Especially for low densities and temperatures the errors become larger than the actual value of the specific heat, and the values are thus omitted in Fig. 5 to enhance the visibility of the overall trends. Indeed c_v approaches $\frac{3}{2}$ for low densities and high temperatures, while being close to 3 for $n = 1$ and low temperatures.

B. Pair correlation function

The pair correlation function $g(r)$ gives insight into the average distance between particles. $g(r)$ can be calculated from a histogram containing the particle pair distances $n(r)$ using

$$g(r) = \frac{2V}{N(N-1)} \left[\frac{\langle n(r) \rangle}{4\pi r^2 \Delta r} \right], \quad (12)$$

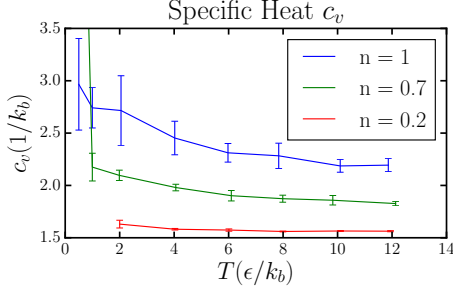


FIG. 3: Specific heat as a function of temperature for various densities. Error bars indicate standard deviations. In the solid phase the specific heat goes to 3 as expected, whereas for lower densities and high temperatures the specific heat converges to the ideal gas result of 1.5.

where Δr is the width of the bins in the histogram.[5] The factor $4\pi r^2$ accounts for the increasing volume of a shell of width Δr in spherical coordinates

In the solid phase, well defined peaks corresponding to the fcc lattice are expected[6]. In the gas phase on the contrary, the interactions are less important and the particles are distributed randomly leading to $g(r) \approx 1$ for $r > \sigma$. This behaviour is observed after the system has equilibrated, as can be seen in Fig. 4. The liquid phase is a transition between these extrema, showing low-amplitude oscillations around $g(r) = 1$.

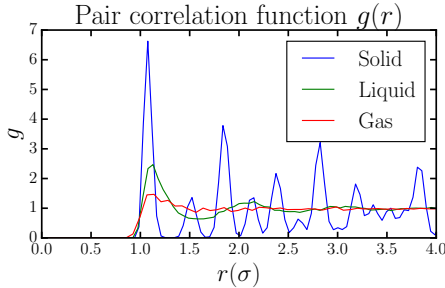


FIG. 4: The pair correlation function for the solid, liquid and gas phase. Following [2] the following values were used: Solid: $T = 0.5$ and $\rho = 1.2$, liquid: $T = 1$ and $\rho = 0.8$, gas: $T = 3$ and $\rho = 0.3$. Results were obtained for $N=864$. The system was equilibrated in 5000 time-steps.

C. Pressure

The pressure is calculated using the Virial theorem:

$$P = \frac{NT}{V} \left[1 - \frac{1}{3NT} \left\langle \sum_i \frac{\partial U}{\partial \mathbf{r}_i} \cdot \mathbf{r}_i \right\rangle \right] \quad (13)$$

Since the total potential energy is built up by two particle interactions, the average $\langle \sum_i \frac{\partial U}{\partial \mathbf{r}_i} \cdot \mathbf{r}_i \rangle$ can be evaluated within the force calculation.

However, the particles which are further than r_{co} apart can also give a significant contribution, as the number of particles at a distance r scales as r^2 . Therefore Eq. 13 is split up into two parts: the first part is evaluated using the force calculation, the other is evaluated analytically.[2]

$$\frac{P}{nT} = 1 - \frac{1}{3NT} \left\langle \sum_i \sum_{j>i} r_{ij} \frac{\partial U(R)}{\partial r_{ij}} \right\rangle_{co} \quad (14)$$

$$- \frac{2\pi N}{3TV} \int_{r_{co}}^{\infty} r^3 \frac{\partial U(r)}{\partial r} g(r) dr$$

The third part of this expression can be evaluated by assuming $g(r) \approx 1$ for $r > r_{co}$. This gives:

$$\int_{r>r_{co}} r^3 g(r) \frac{\partial U}{\partial r} dr \approx 8 \frac{1}{r_{co}^3}, \quad (15)$$

where the r^{-12} term in the Lennard-Jones potential is neglected.

Following Verlet, the pressure is determined for $T = 1, 1.35$ and 2.74 for various densities ρ . These results are plotted in Figure 5. The obtained results resemble those found by Verlet.[1]

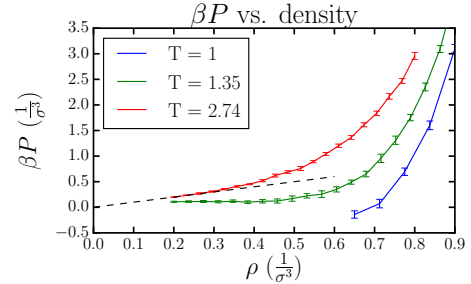


FIG. 5: The pressure as a function of density for various temperatures. The dashed line indicates the ideal gas law. Error bars indicate standard deviations. Results were obtained for $N=500$.

In this figure we can see that for high densities the pressure is higher than would be expected from the ideal gas law. This makes sense as the short

range repulsive interaction increases the pressure. However, at lower densities the intermediate range attraction is more important, and thus the pressure is lower than would be expected from the ideal gas law.

For $T = 1$ the pressure can even become negative. This is caused by the fact that at this temperature it is very favourable for the atoms to be close together. It can even happen that clusters with higher densities and parts with only few particles are formed, which is illustrated in Fig. 6.

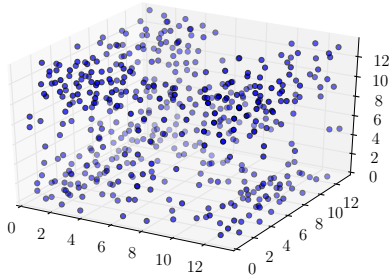


FIG. 6: The final positions of the particles for $T = 1$ and $\rho = 0.2$. Cluster with higher densities can be recognized. Results were obtained for $N=500$ and after 20000 simulation steps.

As can be seen in Fig. 4 the approximation that $g(r) \approx 1$ for $r > r_{co}$ is quite good for gasses and liquids, but it is less accurate for solids. In this case the accuracy of the pressure could be improved by increasing the cut-off length or by using the actual correlation function approximated using Eq. 12.

D. Diffusion

If the motion of a single particle within the gas is tracked as a function of time, then this single particle should show diffusive behaviour in the gaseous and liquid state. Diffusion can be described by the following equation which was derived by Einstein[7]:

$$\langle |\Delta \mathbf{r}|^2 \rangle = 6Dt, \quad (16)$$

where D is the diffusion coefficient and $\Delta \mathbf{r}$ is the difference between the initial position and the position at the time t .

Figure 7 illustrates the diffusive behaviour in the various phases. The diffusion coefficient is highest for the dilute gas, whereas in a liquid the diffusion coefficient is low. In the solid phase $D \approx 0$ as the particle positions are nearly fixed. For times t smaller than the mean free time, ballistic transport will occur and thus $\langle |\Delta \mathbf{r}|^2 \rangle$ scales with t^2 . As a

result, the linear fit does not match the data for small times. This is most clearly visible for the dilute gas.

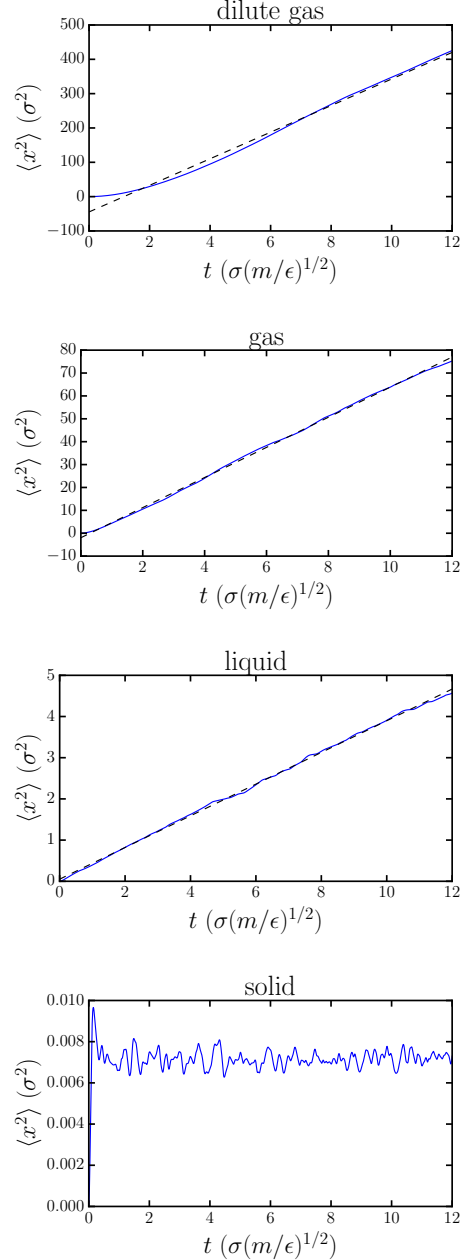


FIG. 7: Mean squared displacement versus time for the various phases. For the dilute gas, $T = 3$ and $\rho = 0.05$ were used, whereas for the other phases the parameters are the same as in Fig. 4. The dashed line indicates the best linear fit. Results were obtained using $N = 500$ particles.

The linear fits led to the diffusion coefficients in Table I. The errors are based on the uncertainty in the linear fit.

TABLE I: Diffusion coefficients for different phases

Phase	T	ρ	D
dilute gas	3.0	0.05	6.45 ± 0.01
gas	3.0	0.3	$1.10 \pm 7 \cdot 10^{-4}$
liquid	1.0	0.8	$0.06 \pm 3.7 \cdot 10^{-5}$

IV. CONCLUSION AND OUTLOOK

In this paper an argon gas interacting via the Lennard-Jones potential has been simulated. The observed results resemble the ideal gas behaviour in the non-interacting limit. Furthermore the gas solidifies at low temperature and high density. The behaviour found in the intermediate regime corresponds well to that found in literature [1, 6]. Thus using computational physics many thermodynamic properties of the system have been correctly determined, which could not have been done using analytical methods. One point of improvement is the approach to determine the specific heat for low temperatures and densities. Longer simulation times and data-blocking lengths should have been used to diminish the errors in the average values.

The model could be expanded in several ways. For example by fixing the pressure instead of the volume, or by moving to the grand canonical ensemble and fix the chemical potential instead of the number of particles. Furthermore processes like phase transitions or hysteresis could be examined. This could reveal even more thermodynamic properties of the Lennard-Jones gas.

Appendix A ERROR SPECIFIC HEAT

The relative fluctuations in the kinetic energy are quite large for small temperatures. As a re-

sult, a long run time is needed in order to obtain an accurate value for the specific heat. Because the errors in the specific heat obtained using data-blocking were quite large, a different error estimation is performed to check these errors.

The heat capacity is given by

$$c_v = \frac{3}{2} \frac{1}{1 - \frac{3N}{2} \frac{\langle \delta K^2 \rangle \pm \epsilon_1}{\langle K \rangle^2 \pm \epsilon_2}} \quad (\text{A.1})$$

We perform a Taylor expansion of the heat capacity, as function of the errors ϵ_1, ϵ_2 , around $\epsilon_1 = \epsilon_2 = 0$, while assuming these (relative) errors to be small so that we only take the errors to first order. This leads to the following expansion

$$\begin{aligned} c_v(\epsilon_1, \epsilon_2) &= c_v(0, 0) + \left. \frac{\partial c_v}{\partial \epsilon_1} \right|_{\epsilon_1, \epsilon_2=0} \epsilon_1 + \left. \frac{\partial c_v}{\partial \epsilon_2} \right|_{\epsilon_1, \epsilon_2=0} \epsilon_2 \\ &+ \mathcal{O}(\epsilon^2) \\ &= c_v(0, 0) + N c_v(0, 0) \frac{\mp \epsilon_1}{\langle K \rangle^2} \\ &+ N c_v(0, 0) \frac{\mp \langle \delta K^2 \rangle \epsilon_2}{\langle K \rangle^4} + \mathcal{O}(\epsilon^2). \end{aligned}$$

Here terms of the form $\epsilon_1 \epsilon_2$ are also considered to be of $\mathcal{O}(\epsilon^2)$. Denoting $E_1 = N c_v(0, 0) \frac{\mp \epsilon_1}{\langle K \rangle^2}$ and $E_2 = N c_v(0, 0) \frac{\mp \langle \delta K^2 \rangle \epsilon_2}{\langle K \rangle^4} + \mathcal{O}(\epsilon^2)$, we find as total error (approximation the errors to be independent) $E_{total} = \sqrt{E_1^2 + E_2^2}$.

When these errors are compared with the errors obtained using data-blocking, they turn out to be of the same order. We can therefore safely conclude that the errors in the specific heat are, although large, estimated correctly.

-
- [1] L. Verlet. Computer "Experiments" on Classical Fluids. I. Thermodynamical Properties of Lennard-Jones Molecules. *Phys. Rev.*, 159(1):98–103, 1967.
 - [2] J.M. Thijssen. *Computational Physics*. Cambridge University Press, Cambridge, Second Edition edition, 2013.
 - [3] O. Lenz. Lennard-jones potential — Wikipedia, the free encyclopedia, 2007. [Online; accessed 11-Februari-2016].
 - [4] D. Mayer. File:cubic-face-centered.svg — Wikipedia, the free encyclopedia, 2007. [Online; accessed 18-Februari-2016].
 - [5] Tildesley D.J. Allen, M.P. *Computer Simulation of Liquids*. Oxford University Press, Oxford, 1989.
 - [6] A. Rahman. Correlations in the Motion of Atoms in Liquid Argon. *Phys. Rev.*, 136(2), 1964.
 - [7] L. Peliti. *Statistical Mechanics in a Nutshell*. Princeton University Press, Princeton, English translation 2011 edition, 2003.